MEDINFO 2021: One World, One Health – Global Partnership for Digital Innovation
P. Otero et al. (Eds.)

doi:10.3233/SHTI220162

Study of 2D Feature Extraction Techniques for Classification of Spinocerebellar Ataxia Type 12 (SCA12)

Snigdha Agrawal[a], Senthil S Kumaran[b], Achal Kumar Srivastava[c], Ramesh Kumar Agrawal[a], Manpreet Kaur Narang[c]

[a] School of Computer and Systems Sciences, Jawaharlal Nehru University, New Delhi, India
[b] Department of MRI and NMR, All India Institute of Medical Sciences, New Delhi, India
[c] Department of Neurology, All India Institute of Medical Sciences, New Delhi, India

Abstract

Spinocerebellar ataxia type 12 (SCA12) is a neurodegenerative genetic disorder triggered by abnormal CAG repeat expansion at locus 5q32. MRI recognises dissimilarities in affected areas of SCA12 patients and healthy subjects. But manual diagnosis is time-consuming and prone to subjective errors. This has motivated us in developing a systematic and authentic decision model for computer-aided diagnosis (CAD) of SCA12. Four different feature extraction techniques are examined in this research work, such as First Order Statistics, GLRLM, GLCM, and GLGCM, to obtain distinguishable characteristics for differentiating SCA12 patients from healthy subjects. The model's performance is measured using sensitivity, specificity, accuracy and F1-score with leave-one-out cross-validation scheme. Our experimental results show that features based on the GLRLM can distinguish SCA12 from healthy subjects with a maximum classification accuracy of 85% among all the different function extraction techniques used.

Keywords:

Spinocerebellar Ataxia, Magnetic resonance imaging, Machine Learning.

Introduction

Spinocerebellar Ataxia (SCA) is a growing neuro-progressive disorder caused by dysfunction of the cerebellum and spinal cord. Damage to the cerebellum can arise as an outcome of injury or illness (acquired ataxia) or because of degeneration of the cerebellum or spinal cord (hereditary ataxia), which mainly causes a lack of motor and speech coordination [7]. The first SCA gene was identified in 1993 and named Spinocerebellar ataxia type 1 (SCA1), while later genes were called SCA2, SCA3, etc. Ataxia is usually caused by damage to the cerebellum, the spinal cord or other nerves [8].

SCA12 was first identified by Holmes et al. [15] in a German-American kindred who had complaints of hand tremor accompanied by symptoms of cerebellar ataxia in later years of life. Affected individuals also developed parkinsonism, psychiatric manifestations, dementia, and autonomic abnormalities in later stages [15]. The number of cases reported worldwide for SCA12 were very scarce [22]. SCA12 being one of the rare subtypes is found chiefly limited to India [1,22,35]. SCA12 is caused by the abnormal CAG repeats expansion in the 5' untranslated region of PPP2R2B gene at locus 5q32 [15].

SCA12 is marked by significant tremors in the arms but can occur in the tongue, lips, neck and trunk [34]. Intentional tremor (tremor with purposeful movements) and postural tremor (tremor at rest) are also detected [26]. Clinical manifestations of SCA12 include cerebellar dysfunctions, generalised hyperreflexia, tremor, gait dysfunction, extrapyramidal features, pyramidal weakness, cognitive and behavioural disturbances [29].

The preliminary diagnosis of SCA12 can be made using Ataxia Rating Scales such as Unified Ataxia Disorders Rating Scale: UADRS [37], The International Cooperative Ataxia Rating Scale: ICARS [38] and Scale for the Assessment and Rating of Ataxia: SARA [33] helped clinicians for initial diagnosis of SCA. A complete neurological evaluation using Genetic testing confirms the presence of ataxia in patients. These clinical evaluation tests are based on the patient's medical or family history. These tests are mostly indirect and biased as they rely on expert clinicians' experience, which may produce subjective findings. Also, information gathering from patients requires a significant amount of time and effort [25].

A new potential for computer-aided diagnosis (CAD) in medicine has been created by brain imaging. Structural Magnetic Resonance Imaging (sMRI) is the most preferred neuroimaging technique among many brain imaging modalities due to its capability to deliver high-resolution anatomic images of brain tissues and the inherent characteristic non-invasiveness.

Severe neuronal loss has been reported in cerebellar hemispheres, vermis, midbrain [9,14,16,22,24,27–30,32,36]. While the studies listed have indicated distinguishable degeneration patterns, there is still a lack of thorough quantitative analysis of degeneration patterns for different subtypes of SCA. Also, limited research work is done on neuroimaging of SCA12. The disease identification is done through genetic testing (Blood test), which takes approximately three months. This is accompanied by an MRI scan which clinicians manually analyse. This makes the whole process of diagnosing the disease long, cumbersome, and susceptible to human error. There have been attempts to apply Machine learning in SCA2, SCA3 and SCA6 [18,19,42,43], but according to our knowledge, no work has been done in SCA12 to date. We explored a few machine learning models in SCA12's structural MRI data to determine its role and efficacy to help the doctors diagnose accurately and quickly. To do so, we need meaningful and distinguishable features to be extracted from raw brain volumes. Therefore, in this work, we investigate four different statistical and texture-based feature extraction methods [2,3,17] to determine their strength in distinguishing SCA12 patients from the control. The obtained characteristic features are ranked, and a minimum set of appropriate features are selected using univariate feature selection. The Support Vector Machine (SVM) is used to construct the decision model for classification. The MRI samples used in

this work has been collected at AIIMS, New Delhi, under the supervision of a senior neurologist and expert radiologist, maintaining the quality of the samples using the standard protocols. This work focuses on extracting features efficiently, developing an effective and authentic decision model for computer aided diagnosis (CAD) of SCA12.

Methods

The proposed model entails four components: Data collection and preprocessing, feature extraction, feature selection, and classification. The given data was preprocessed using SPM12. This was followed by the application of four different Feature Extraction methods in 2D space to extract features. The set of relevant features were then ranked and chosen using FDR. The reduced feature set was then given as an input to the SVM to build decision model.

Data Collection and pre-processing

Subjects

The subjects were recruited from the Neurology Clinics of a referral hospital. The patients were briefed about the study, and they had signed informed consent regarding the complete process of diagnosis before the study. The healthy subjects recruited were free from any known neurological deficits, while the SCA12 recruited subjects lacked any psychological discrepancies, suggesting that the changes in brain volumes were only due to SCA12. The severity of the disease was recorded with the help of The International Cerebellar Ataxia Rating Scale: ICARS score [38] and CAG repeats [15] found in genetic testing. The unpaired two-tailed two-sample t-test was used to infer that the difference between the gender and age of the two groups was insignificant. The details of age, sex, ICARS and CAG Repeat Length are described in Table I.

Table I : Demographic details

	SCA 12 Patients (n=30)	Healthy Controls (n=30)
Males / Females	21M / 9F	21M / 9F
Age Range (in years)	33 - 60	34 - 61
Mean ± Std	49.4 ± 7.9	49.4 ± 7.8
TIV (in cm^3)	1309.9 ± 102.7	1280.43 ± 99.9
ICARS Score	28.63 ± 9.3	-
Age at Onset (in years)	45.76 ± 7.8	-
CAG Repeat Length	56.83 ± 5.4	-

Data Acquisition

The 60 subjects: 30 controls (age: 49.4 ± 7.8), were without any previously known neurological deficits, and 30 SCA12 patients (age ± SD = 49.4 ± 7.9, range: 33 to 60) were recruited. The structural MRI data was acquired in a 3 T MR scanner (Ingenia, M/s Philips Healthcare) using 3D TFE T1 weighted sequence consisting of 350 slices, in sagittal orientation slices (of 1 mm acquired voxel size with -0.5 mm slice thickness, so that the reconstructed voxel size was 0.5 X 0.5 X 0.5mm3), TR/ TE: 8.1/3.7 ms, echo spacing: 8.6 ms, FOV: 240 mm2 using a 32-channel head coil with the subject in the supine position and restrained head to avoid any head movement. T2 (3D T2 FFE) was also acquired to rule out any morphological deficit (other than for SCA in patients). In general, morphological deficits or artifacts are observed in excessive motion cases. To verify their absence, all the brain images were checked by an expert radiologist.

Data Pre-Processing

For each anatomical image, the brain MRI images were converted from DICOM (Digital Imaging and Communications in Medicine) to 3D Neuroimaging Informatics Technology Initiative (Nifti) format using MRIcron (dcm2nii) [44]. Each T1 volume was manually reoriented using the Display option in Statistical Parametric Mapping (Ver. SPM12, v4667) software (Friston et al., 2005) on MATLAB platform (R2019a; The Math Works, Natick, MA, USA) to set the origin (0,0,0 coordinates) along the anterior commissure (AC) – posterior commissure (PC) line. After manual reorientation, all the images were preprocessed using expert mode in CAT12 (Computational Anatomy Toolbox) [11] of SPM12. The steps followed were according to the CAT12 manual [11]. The T1 images were normalised to the space of MNI template and then segmented into gray matter (GM), white matter (WM) and cerebrospinal fluid (CSF).

Feature Extraction

A feature may be defined as a discriminative, informative, and independent aspect, quality or attribute that may be representative or numeric. In the case of medical diagnosis, the features can be considered a pattern responsible for the disease or symptoms, a set of variables cataloguing the health conditions of a patient (e.g. fever, glucose level, etc.) [12]. The raw MRI volume is usually characterised by a massive number of features (voxels). Some of these (mostly those closer to blood vessels) may be noisy, redundant, and irrelevant. The presence of such features may deteriorate the recital of the decision system. In machine learning, we initially find a minimal set of relevant features, which can distinguish two different kinds of patterns more effectively and improve the generalisation and interpretability of the decision system.

Feature extraction is one method for reducing dimensionality, representing the data in another space to find a more meaningful and compact representation of the data. Since the features extracted contain relevant information, the task can be performed on this reduced set of features rather than the original dataset [20]. This helps reduce memory usage and computation time and enables us to overcome the situation when a classification method may lead to overfitting of training data.

Some popular feature extraction techniques like First Order Statistics (FO), Gray Level Co-occurrence Matrix (GLCM), Gray Level Gradient Co-occurrence Matrix (GLGCM), Gray Level Run Length Matrix (GLRLM), etc. have been investigated in this work to find its suitability in distinguishing SCA12 from the control.

First Order Statistics

First-order statistics define the spread of voxel intensities within the image region using frequently used metrics like mean, median, mode, standard deviation, kurtosis, skewness, and mean average deviation. These measures are well known and commonly used.

First-order statistics is employed on each 2D slice of the subject's brain volume individually to obtain seven features. The features so obtained from all slices of a given volume are averaged to form a feature vector for each measure. Each of these measures is then concatenated to represent the volume. After the features are extracted using first-order statistics for all the

subjects (patients and healthy controls), the feature set is normalised so that the range is between 0 to 1. The method is named First_Order.

Gray Level Co-occurrence Matrix

The gray level co-occurrence matrix (GLCM) captures second-order statistics where spatial relation between pairs of pixels with respect to each other are studied [17]. For this, (i, j)th element of co-occurrence matrices corresponds to the number of occurrences of a pixel with intensity A_i at a distance d from another pixel with intensity A_j in the direction θ. Haralick and Shanmugam [13] proposed 14 measures to condense these matrices to a few numbers to represent a given texture. Out of the 14 measures, we exclude the Maximal Correlation Coefficient due to computational instability [39].

2D GLCM is employed on each slice of the subject's brain volume individually to obtain 13 features for each of the four directions, i.e., 0,45,90,135. The features obtained from all the slices of a given volume are added. For each of the 13 features, the mean and range are computed from the four directions. The mean and range of features are concatenated to form a 1-dimensional feature vector (total 26 features) corresponding to GLCM feature extraction step. After the features are extracted using GLCM for all the subjects (patients and healthy controls), the feature set is normalised so that the range is between 0 to 1. This whole process is carried out for three different gray levels: 8, 16, 32. Thus, the methods are named GLCM_8, GLCM_16, GLCM_32.

Gray Level Gradient Co-occurrence Matrix

Gray level gradient co-occurrence matrix (GLGCM) is a variant of co-occurrence matrix that focusses on capturing the second-order statistics of gray level gradient. Though both GLCM and GLGCM concentrates on capturing the second-order statistics of local image features but GLCM concentrates only on capturing the second-order statistics of gray level values while GLGCM captures second-order statistics of gray level gradients [23]. The 13 Haralick features as described above are computed from GLGCM.

2D GLGCM is similar to 2D GLCM. First, we calculate the image gradient of the 2D slice and then employ GLCM on each slice gradient of the subject's brain volume individually to obtain 13 features. The features obtained from all the slices of a given volume are added. These features are added together to find the mean and range of 13 features across the slices for each slice. The mean and range of features are concatenated to form a 1-dimensional feature vector (total 26 features) corresponding to GLCM feature extraction step. After the features are extracted using GLGCM for all the subjects (patients and healthy controls), the feature set is normalised so that the range is between 0 to 1. This whole process is carried out for three different gray levels: 8, 16, 32. Thus, the methods are named GLGCM_8, GLGCM_16, GLGCM_32.

Gray Level Run Length Matrix

Gray Level Run Length Matrix (GLRLM) captures higher-order statistics where spatial relation between pairs of pixels with respect to each other are studied. For this, we construct matrices by finding the number of occurrences of a consecutive number of pixels of length l having the same intensity I in the same direction. Initially, Galloway [10] introduced the concept of GLRLM but with a limited number of features which made this method less efficient compared to others [4,17,40]. Tang [41] proposed new features making it more efficient. A total of 11 features are used to condense these matrices to a few numbers to represent texture.

2D GLRLM is employed on each slice of the subject's brain volume individually to obtain 11 features. The features obtained from all the slices of a given volume are added. For each slice, these features are added together to find 11 features across the slices for each of the four directions i.e., 0,45,90,135. The features obtained from each direction are then concatenated to form a 1-dimensional feature vector (total 44 features) corresponding to GLRLM feature extraction step. After the features are extracted using GLRLM for all the subjects (patients and healthy controls), the feature set is normalised so that the range is between 0 to 1. This whole process is carried out for three different gray levels: 8, 16, 32. Thus, the methods are named GLRLM_8, GLRLM_16, GLRLM_32.

Feature Selection

Only a subset of features might be relevant from the extracted set of features, while the rest might either be irrelevant, redundant, or noisy. The feature selection techniques aim to define a feature subset of relevant features by eradicating redundant, irrelevant and noisy features without degrading performance [21]. Advantages of feature selection include dimensionality reduction of the feature space, decreased computation time, improvement in data visualisation, and an increase in classification accuracy of the resulting decision model.

The feature selection techniques may be classified as (a) the filter methods and (b) the wrapper methods. The former does not depend on the learning algorithms. In filter methods, we assign a score to feature(s). Then these features are ranked based on their scores. This ranking may be used to select or eliminate a given feature from the given set of features. The wrapper methods utilise a classifier to evaluate a subset of features.

The filter methods may further be classified into the univariate and the multivariate selection methods. In the former score is assigned to each feature. Conversely, the multivariate feature selection method considers correlation to select the minimal subset of pertinent, essential, and non-redundant features. This study employs Fisher Discriminant Ratio (FDR), a univariate feature selection technique for choosing the features, which is computationally simple.

Classification

The dataset containing the chosen features serves as an input to the classifier. It is distributed into two fragments: the training and the testing data. Training data is used to build the decision model. It is a supervised learning approach in which a decision model assigns a class label to a new observation (test sample) [6,31]. This study employs Support Vector Machine (SVM) [5] for classification. The performance of the decision system is found using Leave-one out cross-validation (LOOCV) scheme. In each fold of this scheme, one sample is used as testing data while the rest of the samples are used as training data for the classifier. Therefore, the number of samples determine the number of folds in this scheme. This decision model is constructed starting with the first selected pertinent feature. To discover the effect of several features on classification accuracy of the decision model, the features are incrementally included in the order of relevance in building decision model.

Performance Evaluation Parameters

The performance measures, namely sensitivity, specificity, accuracy, and F1-score, have been used to estimate the model's effectiveness. Accuracy is the ratio between the true forecasts and the total number of samples. The sensitivity tests how well positive cases (SCA12 patients) are properly identified by a decision model from actual positive cases, i.e. all SCA12 patients

in practice. Specificity tests the sufficiently categorised negative cases (positive controls) out of the total negative cases, i.e. all healthy cases. The F1-score is the harmonic mean of precision and recall.

Results

Variation of classification accuracy with the number of features for GM volume has been shown in Figure 1. The graph shows the variations for features crafted from 10 different feature extraction methods namely First_Order, GLCM_8, GLCM_16, GLCM_32, GLGCM_8, GLGCM_16, GLGCM_32, GLRLM_8, GLRLM_16 and GLRLM_32.

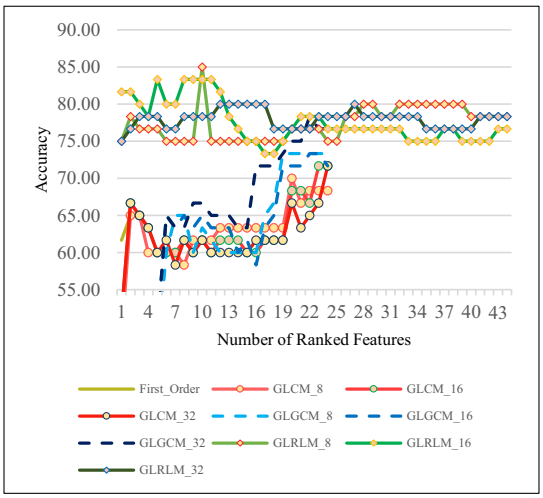

Figure 1: Variation of Classification Accuracy for all Feature Extraction Methods used

The classification accuracy, sensitivity, specificity, precision and F1-score obtained from data for different feature extraction methods is reported in Table II. The best performance value in the Table is shown in bold.

Table II: Classification performance measures for the proposed model

FE	Gray level	Accuracy	Sensitivity	Specificity	F1-Score
First Order Statistics		65	65.52	64.52	64.41
GLCM	8	70	75	66.67	66.67
	16	71.67	76	68.57	69.09
	32	71.67	76	68.57	69.09
GLGCM	8	73.33	75	71.88	72.41
	16	73.33	75	71.88	72.41
	32	78.33	81.48	75.76	77.19
GLRLM	8	85	81.82	88.89	85.71
	16	83.33	81.25	85.71	83.87
	32	80	78.13	82.14	80.65

Discussion

We can draw the following observations from Figure 1 and Table II:

- The GLRLM_8 method performs the best on this given data set for all the four performance measures used.
- As can be observed from the figures that for all the methods, with the increase in the number of features there is an improvement in their accuracy, but it fluctuates after a particular number of features. Among all the methods GLCM_32 and GLGCM_32 have an incrementing graph, thus being more stable.
- The GLRLM (all cases) performs better in classification Accuracy, Specificity and F1-Score concerning other methods.
- In general, the GLCM, GLGCM and GLRLM methods perform better than first-order statistics. We can consider neighbourhood information in these methods that are not captured in first-order statistics. GLRLM performs better as it captures higher-order statistics where it considers the immediate neighbourhood and a larger neighbourhood, which helps capture better statistics.

For second-order statistics, higher gray level yields better results, but for higher-order statistics, the performance deteriorates.

Since no machine learning method has been applied to date to distinguish SCA12 and control to best of our knowledge, we cannot compare our result.

Conclusions

The diagnosis of Spinocerebellar Ataxia Type 12 using automated methods has become the need of the hour, as the manual assessment of the disease requires more time, resources, and expertise. This work proposes a model which uses data consisting of the sMRI images of 30 healthy and 30 SCA12 patients. The proposed model uses four different Feature Extraction methods to extract features from the given data. A univariate technique called FDR is used to select a set of pertinent features with reduced time complexity. This results in a reduced set of essential features. To craft a decision model to distinguish between healthy and SCA12 patients, SVM was used. The performance of the model was gauged via accuracy, sensitivity, specificity, and F1-score. It was observed that using higher-order statistics, we were able to differentiate SCA12 from controls. GLRLM with gray level 8 and followed by feature selection using FDR provides better performance in terms of all four measures compared to existing methods. In future, this work can be extended to 3D Feature extraction methods where we can capture better neighbourhood information to construct a more relevant and minimal set of features to distinguish SCA12 from the control.

Acknowledgements

The authors extend their gratitude to the University Grants Commission, India, to dispense financial support in this research work. Furthermore, authors are highly thankful to All India Institute of Medical Sciences, New Delhi, India, for the valuable contribution in the research.

References

[1] S. Bahl, K. Virdi, U. Mittal, M.P. Sachdeva, A.K. Kalla, S.E. Holmes, E. O'Hearn, R.L. Margolis, S. Jain, A.K. Srivastava, and M. Mukerji, Evidence of a Common Founder for SCA12 in the Indian Population, *Ann. Hum. Genet.* **69** (2005) 528–534. doi:https://doi.org/10.1046/j.1529-8817.2005.00173.x.

[2] G. Castellano, L. Bonilha, L.M. Li, and F. Cendes, Texture analysis of medical images, *Clin. Radiol.* **59** (2004) 1061–1069. doi:10.1016/j.crad.2004.07.008.

[3] C.L. Chowdhary, and D.P. Acharjya, Segmentation and Feature Extraction in Medical Imaging: A Systematic Review, *Procedia Comput. Sci.* **167** (2020) 26–36. doi:10.1016/j.procs.2020.03.179.

[4] R.W. Conners, and C.A. Harlow, A Theoretical Comparison of Texture Algorithms, *IEEE Trans. Pattern Anal. Mach. Intell.* **PAMI-2** (1980) 204–222. doi:10.1109/TPAMI.1980.4767008.

[5] N. Cristianini, and J. Shawe-Taylor, An introduction to support vector machines and other kernel-based learning methods, Cambridge university press, 2000.

[6] R.O. Duda, P.E. Hart, and D.G. Stork, Pattern classification, John Wiley & Sons, 2012.

[7] A.M. Dueñas, R. Goold, and P. Giunti, Molecular pathogenesis of spinocerebellar ataxias, *Brain*. **129** (2006) 1357–1370. doi:10.1093/brain/awl081.

[8] A. Durr, Autosomal dominant cerebellar ataxias: polyglutamine expansions and beyond, *Lancet Neurol.* **9** (2010) 885–894. doi:10.1016/S1474-4422(10)70183-6.

[9] H. Fujigasaki, I.C. Verma, A. Camuzat, R.L. Margolis, C. Zander, A.-S. Lebre, L. Jamot, R. Saxena, I. Anand, S.E. Holmes, C.A. Ross, A. Dürr, and A. Brice, SCA12 is a rare locus for autosomal dominant cerebellar ataxia: A study of an Indian family, *Ann. Neurol.* **49** (2001) 117–121. doi:https://doi.org/10.1002/1531-8249(200101)49:1<117::AID-ANA19>3.0.CO;2-G.

[10] M.M. Galloway, and G. MM, Texture analysis using gray level run lengths., (1975).

[11] C. Gaser, and R. Dahnke, CAT-a computational anatomy toolbox for the analysis of structural MRI data, *HBM.* **2016** (2016) 336–348.

[12] I. Guyon, and A. Elisseeff, An introduction to variable and feature selection, *J. Mach. Learn. Res.* **3** (2003) 1157–1182.

[13] R.M. Haralick, K. Shanmugam, and I. Dinstein, Textural Features for Image Classification, *IEEE Trans. Syst. Man Cybern.* **SMC-3** (1973) 610–621. doi:10.1109/TSMC.1973.4309314.

[14] S.E. Holmes, E. O'Hearn, and R.L. Margolis, Why is SCA12 different from other SCAs?, *Cytogenet. Genome Res.* **100** (2003) 189–197. doi:10.1159/000072854.

[15] S.E. Holmes, E.E. O'Hearn, M.G. McInnis, D.A. Gorelick-Feldman, J.J. Kleiderlein, C. Callahan, N.G. Kwak, R.G. Ingersoll-Ashworth, M. Sherr, A.J. Sumner, A.H. Sharp, U. Ananth, W.K. Seltzer, M.A. Boss, A.-M. Vieria-Saecker, J.T. Epplen, O. Riess, C.A. Ross, and R.L. Margolis, Expansion of a novel CAG trinucleotide repeat in the 5′ region of PPP2R2B is associated with SCA12, *Nat. Genet.* **23** (1999) 391–392. doi:10.1038/70493.

[16] T. Hu, B. Zhao, Q. Wei, and H. Shang, Unusual cerebral white matter change in a Chinese family with Spinocerebellar ataxia type 12, *J. Neurol. Sci.* **349** (2015) 243–245. doi:10.1016/j.jns.2014.12.045.

[17] A. Humeau-Heurtier, Texture Feature Extraction Methods: A Survey, *IEEE Access*. **7** (2019) 8975–9000. doi:10.1109/ACCESS.2018.2890743.

[18] B.C. Jung, S.I. Choi, A.X. Du, J.L. Cuzzocreo, Z.Z. Geng, H.S. Ying, S.L. Perlman, A.W. Toga, J.L. Prince, and S.H. Ying, Principal component analysis of cerebellar shape on MRI separates SCA types 2 and 6 into two archetypal modes of degeneration, *The Cerebellum*. **11** (2012) 887–895.

[19] B.C. Jung, S.I. Choi, A.X. Du, J.L. Cuzzocreo, H.S. Ying, B.A. Landman, S.L. Perlman, R.W. Baloh, D.S. Zee, and A.W. Toga, MRI shows a region-specific pattern of atrophy in spinocerebellar ataxia type 2, *The Cerebellum*. **11** (2012) 272–279.

[20] Y. Kodratoff, Introduction to Machine Learning - 1st Edition, (n.d.). https://www.elsevier.com/books/introduction-to-machine-learning/kodratoff/978-0-08-050930-3 (accessed November 18, 2020).

[21] R. Kohavi, and G.H. John, Wrappers for feature subset selection, *Artif. Intell.* **97** (1997) 273–324.

[22] D. Kumar, A.K. Srivastava, M. Faruq, and V.R. Gundluru, Spinocerebellar ataxia type 12: An update, *Ann. Mov. Disord.* **2** (2019) 48. doi:10.4103/AOMD.AOMD_5_19.

[23] S.W.- Lam, Texture feature extraction using gray level gradient based co-occurence matrices, in: 1996 IEEE Int. Conf. Syst. Man Cybern. Inf. Intell. Syst. Cat No96CH35929, 1996: pp. 267–271 vol.1. doi:10.1109/ICSMC.1996.569778.

[24] H. Li, J. Ma, and X. Zhang, Diffusion tensor imaging of spinocerebellar ataxia type 12, *Med. Sci. Monit. Int. Med. J. Exp. Clin. Res.* **20** (2014) 1783.

[25] E. Lindsay, and E. Storey, Cognitive Changes in the Spinocerebellar Ataxias Due to Expanded Polyglutamine Tracts: A Survey of the Literature, *Brain Sci.* **7** (2017) 83. doi:10.3390/brainsci7070083.

[26] R.L. Margolis, S.E. Holmes, A.K. Srivastava, M. Mukherji, and K.K. Sinha, Spinocerebellar Ataxia Type 12 – RETIRED CHAPTER, FOR HISTORICAL REFERENCE ONLY, in: M.P. Adam, H.H. Ardinger, R.A. Pagon, S.E. Wallace, L.J. Bean, K. Stephens, and A. Amemiya (Eds.), GeneReviews®, University of Washington, Seattle, Seattle (WA), 1993. http://www.ncbi.nlm.nih.gov/books/NBK1202/ (accessed November 22, 2020).

[27] E. O'Hearn, O. Pletnikova, S. Holmes, J. Trojanowski, R. Margolis, and J. Troncoso, SCA12 neuropathology: Cerebral cortical and cerebellar atrophy, Purkinje cell loss, and neuronal intranuclear inclusions., in: WILEY-LISS DIV JOHN WILEY & SONS INC, 111 RIVER ST, HOBOKEN, NJ 07030 USA, 2004: pp. 1124–1125.

[28] E.E. O'Hearn, H.S. Hwang, S.E. Holmes, D.D. Rudnicki, D.W. Chung, A.I. Seixas, R.L. Cohen, C.A. Ross, J.Q. Trojanowski, O. Pletnikova, J.C. Troncoso, and R.L. Margolis, Neuropathology and Cellular Pathogenesis of Spinocerebellar Ataxia Type 12, *Mov. Disord.* **30** (2015) 1813–1824. doi:https://doi.org/10.1002/mds.26348.

[29] E. O'Hearn, S. Holmes, P.C. Calvert, C.A. Ross, and R.L. Margolis, SCA-12: tremor with cerebellar and cortical atrophy is associated with a CAG repeat expansion, *Neurology*. **56** (2001) 299–303.

[30] E. O'Hearn, S.E. Holmes, and R.L. Margolis, Spinocerebellar ataxia type 12, in: Handb. Clin. Neurol., Elsevier, 2012: pp. 535–547.

[31] H. Peng, F. Long, and C. Ding, Feature selection based on mutual information criteria of max-dependency, max-relevance, and min-redundancy, *IEEE Trans. Pattern Anal. Mach. Intell.* **27** (2005) 1226–1238.

[32] J. Rossi, F. Cavallieri, G. Giovannini, C. Budriesi, A. Gessani, M. Carecchio, D. Di Bella, E. Sarto, J. Mandrioli, and S. Contardi, Spasmodic dysphonia as a presenting symptom of spinocerebellar ataxia type 12, *Neurogenetics*. **20** (2019) 161–164.

[33] T. Schmitz-Hübsch, S.T. Du Montcel, L. Baliko, J. Berciano, S. Boesch, C. Depondt, P. Giunti, C. Globas, J. Infante, and J.-S. Kang, Scale for the assessment and rating of ataxia: development of a new clinical scale, *Neurology*. **66** (2006) 1717–1720.

[34] K. Sinha, and J. Desai, Hereditary Ataxias, *Neurol. Pract. Indian Perspect.* (2005) 409.

[35] A.K. Srivastava, S. Choudhry, M.S. Gopinath, S. Roy, M. Tripathi, S.K. Brahmachari, and S. Jain, Molecular and clinical correlation in five Indian families with spinocerebellar ataxia 12, *Ann. Neurol.* **50** (2001) 796–800. doi:https://doi.org/10.1002/ana.10048.

[36] A.K. Srivastava, A. Takkar, A. Garg, and M. Faruq, Clinical behaviour of spinocerebellar ataxia type 12 and intermediate length abnormal CAG repeats in PPP2R2B, *Brain*. **140** (2017) 27–36.

[37] S. Subramony, W. May, D. Lynch, C. Gomez, K. Fischbeck, M. Hallett, P. Taylor, R. Wilson, and T. Ashizawa, Measuring Friedreich ataxia: interrater reliability of a neurologic rating scale, *Neurology*. **64** (2005) 1261–1262.

[38] P. Trouillas, T. Takayanagi, M. Hallett, R.D. Currier, S.H. Subramony, K. Wessel, A. Bryer, H.C. Diener, S. Massaquoi, C.M. Gomez, P. Coutinho, M.B. Hamida, G. Campanella, A. Filla, L. Schut, D. Timann, J. Honnorat, N. Nighoghossian, and B. Manyam, International Cooperative Ataxia Rating Scale for pharmacological assessment of the cerebellar syndrome, *J. Neurol. Sci.* **145** (1997) 205–211. doi:10.1016/S0022-510X(96)00231-6.

[39] A. Uppuluri, GLCM texture features, *MATLAB Cent. File Exch.* (n.d.). https://in.mathworks.com/matlabcentral/fileexchange/22187-glcm-texture-features (accessed December 6, 2020).

[40] J.S. Weszka, C.R. Dyer, and A. Rosenfeld, A Comparative Study of Texture Measures for Terrain Classification, *IEEE Trans. Syst. Man Cybern.* **SMC-6** (1976) 269–285. doi:10.1109/TSMC.1976.5408777.

[41] Xiaoou Tang, Texture information in run-length matrices, *IEEE Trans. Image Process.* **7** (1998) 1602–1609. doi:10.1109/83.725367.

[42] Z. Yang, S.M. Abulnaga, A. Carass, K. Kansal, B.M. Jedynak, C. Onyike, S.H. Ying, and J.L. Prince, Landmark based shape analysis for cerebellar ataxia classification and cerebellar atrophy pattern visualisation, in: Med. Imaging 2016 Image Process., International Society for Optics and Photonics, 2016: p. 97840P. doi:10.1117/12.2217313.

[43] Z. Yang, C. Ye, J.A. Bogovic, A. Carass, B.M. Jedynak, S.H. Ying, and J.L. Prince, Automated cerebellar lobule segmentation with application to cerebellar structural analysis in cerebellar disease, *NeuroImage*. **127** (2016) 435–444. doi:10.1016/j.neuroimage.2015.09.032.

[44] dcm2nii DICOM to NIfTI conversion, (n.d.). https://people.cas.sc.edu/rorden/mricron/dcm2nii.html (accessed November 18, 2020).

Address for correspondence

Snigdha Agrawal : snigdhaagrawal.1992@gmail.com, +91-9968954972